Journal Computer and Technology
Vol. 4, No. 1, July 2026, pp. 61-75
ISSN: 3048-1880 (Online)
DOI: https://doi.org/10.69916/comtechno.v4i1.408

OPEN ACCESS

Original Research

Beyond Intensity Gradients: A Lightweight Client-Side Morphological Framework for Robust Binary Image Segmentation

Gregorius Ananta Sinaga[1], Haida Dafitri[*2]

[1,2] Department of Informatics, Faculty of Engineering and Computer Science, Universitas Harapan Medan
Email: [1]gregorius.ananta@gmail.com, [2]aida.stth@gmail.com

ARTICLE HISTORY
Received: December 22, 2025
Revised: July 14, 2026
Published: July 22, 2026

Copyright © 2026 by the Authors: This is an open-access article distributed under the terms of the Creative Commons Attribution 4.0 International License.

ABSTRACT

Edge detection in binary images frequently suffers from contour fragmentation when utilizing conventional gradient operators (e.g., Sobel, Canny), as they inherently rely on continuous intensity variations absent in discrete binary data. To address this, this study proposes a lightweight, client-side morphological gradient framework designed to structurally and topologically extract object boundaries based purely on spatial geometry. A modular web-based computational pipeline was developed using a PHP-JavaScript architecture, integrating adaptive Otsu binarization, dynamic kernel configurations, and core morphological computations. For rigorous algorithmic and engineering validation, the system was benchmarked against the conventional Canny detector using a dataset of 50 botanical images, supplemented by comprehensive white-box and black-box software testing involving 20 participants across 20 distinct test cases. Experimental results demonstrate that the proposed morphological framework achieves superior topological fidelity and boundary continuity. It secured an optimal F1-score of 0.9006 using a 3×3 disk structuring element, significantly outperforming the Canny detector's F1-score of 0.7761. Furthermore, the method exhibits highly parallelizable efficiency, executing edge extraction at a mean runtime of 18.2 ms, more than twice as fast as the multi-stage Canny operator (42.5 ms). Software evaluations confirmed exceptional system reliability, yielding a 97.4% functional success rate, 95% overall module coverage, and an excellent usability score of 4.58/5.0. Ultimately, this research proves that shifting the paradigm from intensity differentiation to mathematical morphology offers a highly precise, robust, and computationally lightweight solution for real-time, web-native binary image segmentation.

Keyword: Image Segmentation; Edge Detection; Morphological Gradient; Binary Image; Performance Metrics.

How to Cite:
G. A. Sinaga and H. Dafitri, "Beyond Intensity Gradients: A Lightweight Client-Side Morphological Framework for Robust Binary Image Segmentation," *J. Comput. Technol.*, vol. 4, no. 1, pp. 62–76, 2026.

1. INTRODUCTION

Image segmentation is a fundamental step in digital image processing, aiming to partition an image into multiple homogeneous regions based on specific characteristics such as intensity, color, or texture. The accuracy of this segmentation critically dictates the quality of downstream outcomes across diverse applications, ranging from pattern recognition to medical image analysis. However, in practical scenarios, segmentation frequently encounters challenges, including ill-defined object boundaries, the presence of noise, and low contrast between the foreground and background. These issues collectively degrade the overall accuracy of object identification and comprehensive feature extraction [1]. A widely employed technique to facilitate segmentation is edge detection, a method designed to identify abrupt changes in pixel intensity that signify object boundaries. In the context of binary images, which possess only two discrete intensity values, edge detection becomes particularly paramount due to the severe limitation of available visual information. Binary images are extensively utilized in applications such as optical character recognition (OCR), document analysis, and cellular segmentation, all of which demand high precision in contour delineation. Consequently, the efficacy of edge detection in binary imagery directly dictates the overall success and reliability of the subsequent segmentation process [2].

While prior studies have advanced edge detection and segmentation, each method exhibits inherent limitations across diverse image characteristics, as detailed below, the study in [3] proposed a color image segmentation algorithm based on the watershed transform and morphological gradient. The primary advantage of this approach

lies in its robustness against specular reflections, effectively suppressing meaningless regions while achieving an accuracy and recall rate exceeding 0.98. Nevertheless, its limitation stems from a heavy reliance on color space transformation (RGB to YCbCr) and multi-scale reconstruction, which inadvertently risks attenuating original edge information. Furthermore, the methodology is not optimized for binary image processing. Building upon this, the research in [3] developed a morphological gradient-based watershed algorithm integrated with a region-growing technique for color images. The principal strength of this method is the independent extraction of intensity and texture gradients prior to fusion, thereby yielding more precise object boundaries. However, its scope is strictly confined to color imagery. Additionally, its dependence on the region-growing process necessitates initial seed selection, which increases computational complexity and reduces efficiency for straightforward image processing tasks. Conversely, the study in [4] explored the utilization of gradient magnitude coupled with the Robert's Cross operator for edge detection in grayscale images. The notable advantage of this research is its efficacy in elucidating patterns and object boundaries in high-contrast scenarios. Despite this, the method exhibits a critical limitation, evidenced by a classification accuracy of merely 75%. It also demonstrates poor robustness against high-noise environments and low-contrast imagery, as its edge detection performance is highly susceptible to errors stemming from manual threshold adjustments. In a comprehensive survey, [5] highlighted the evolution of edge detection utilizing deep learning architectures, including CNNs, Transformers, and generative models. The paramount advantage of these deep learning paradigms is their exceptional precision (e.g., achieving an Optimal Dataset Scale [ODS] > 0.87) in capturing global contexts and intricate features. Nevertheless, their primary drawbacks encompass severe computational overhead, architectural complexity, and the prerequisite for massive training datasets. Consequently, these models lack the practicality and adaptability required for direct application to binary images, which inherently possess only two discrete intensity values. Focusing specifically on gradient reconstruction, the study in [3] emphasized the critical role of morphological opening and closing operations in reconstructing gradient images prior to segmentation. The strength of this reconstruction technique lies in its capacity to filter out fine-texture noise while preserving the primary contours of the object. Despite this merit, a significant limitation is that the filtering process may inadvertently blur subtle edge information (*soft edges*). This issue becomes particularly critical when applied to binary images, which entirely lack continuous intensity gradients. Most recently, the research in [6] integrated morphological closing operations with adaptive thresholding for the segmentation of medical fingernail images. The primary advantage of this method is its efficacy in bridging minor gaps within detected edges and eliminating noise artifacts, thereby achieving exceptionally high accuracy and Intersection over Union (IoU) scores (exceeding 0.95) with computational efficiency. However, its limitation lies in its heavy reliance on predefined parameters, such as the morphological kernel size. Furthermore, its highly specific focus on medical imagery raises questions regarding its flexibility and generalizability for pure contour extraction in general binary images.

Synthesizing the aforementioned literature, it is evident that the majority of existing edge detection approaches predominantly focus on continuous color or grayscale intensity variations, complex deep learning architectures [7], or highly specific offline medical applications. A conspicuous gap remains: conventional gradient-based operators (e.g., Sobel, Prewitt, and Canny) remain fundamentally suboptimal for discrete binary images characterized by fine contours or micro-scale structures [8]. Their inherent reliance on spatial intensity derivatives renders them highly sensitive to noise and prone to contour fragmentation when encountering the extreme-contrast, step-edge nature of binary data. Furthermore, integrating complex edge detection frameworks into modern distributed systems often incurs severe computational overhead, limiting their viability for real-time web deployment.

To bridge these critical gaps, this study introduces an optimized, web-native morphological gradient framework explicitly engineered for robust client-side binary image segmentation [9]. By shifting the paradigm from intensity differentiation to mathematical morphology, the proposed method leverages localized spatial geometry through dynamic structuring elements to extract continuous, topologically cohesive object boundaries without the necessity of heavy external libraries. This lightweight framework not only inherently mitigates the "broken edges" dilemma under discrete constraints but also minimizes the computational footprint to a millisecond-level execution. Consequently, this research provides a highly precise, low-latency computational pipeline tailored for resource-constrained architectures demanding rigorous structural fidelity.

2. RESEARCH METHODS

This study employs a computational approach by designing a web-based modular pipeline to implement and evaluate binary image edge detection using the morphological gradient. Overall, the research methodology is divided into four main stages: data preparation and image preprocessing, morphological gradient algorithm implementation, web-based system design, and testing and evaluation methods.

2.1. Research Flow and Image Preprocessing

The initial stage begins with the collection of test images (e.g., RGB-formatted daisy flower images) exhibiting clear contrast differences between the object and the background. The input images then undergo a preprocessing stage comprising: Grayscale Conversion: Transforming the RGB image into a grayscale image to simplify pixel intensity computation. Binarization (Thresholding): Converting the grayscale image into a binary image (values of 0 and 1, or black and white) [10], [11], [12]. This process utilizes two thresholding approaches: an automatic method (Otsu) and a manual method (user-defined threshold values ranging from 0 to 255) to separate the foreground object from the background.

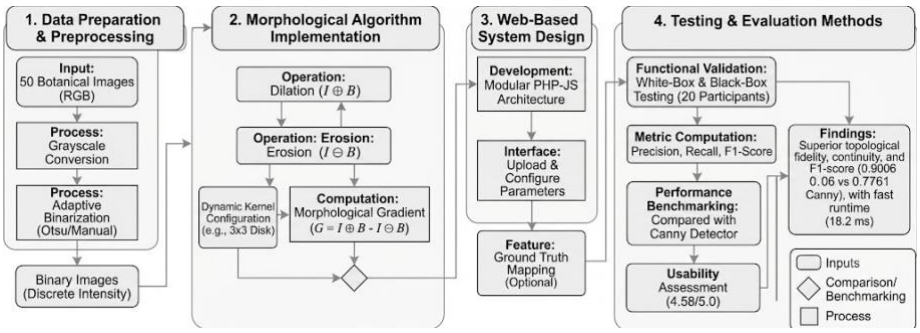


Figure 1. Research Flow of the Morphological Gradient-Based Image Segmentation System

Figure 1 illustrates the comprehensive research methodology deployed in this study, which is divided into four main operational phases to robustly extract binary object edges using the morphological gradient. The pipeline starts with the Data Preparation & Preprocessing phase, where an input dataset comprising 50 botanical RGB images is collected. These color images are first converted into grayscale to eliminate hue complexity and facilitate raw pixel intensity calculations. Following this, adaptive binarization thresholding, utilizing either Otsu's automatic calculation or manual adjustments between 0 and 255, is implemented to create discrete binary images where the foreground object is clearly isolated from the background in absolute black and white states. The next step is the Morphological Algorithm Implementation, which serves as the computational core of the research. The discrete binary image matrix undergoes fundamental mathematical morphology operations: dilation to structurally expand shape boundaries and erosion to structurally shrink them [13].

The Morphological Algorithm Implementation drives boundary extraction using a dynamic kernel configuration with a symmetric 3×3 disk structuring element. The final edge map is computed by taking the absolute mathematical difference between the dilated and eroded images ($G = I \oplus B - I \ominus B$), isolating continuous, single-pixel-width contours without continuous intensity derivatives. The architecture then transitions into the Web-Based System Design phase, where the localized native workflow is integrated into a lightweight client-side dashboard using PHP and JavaScript for real-time image uploads, parameter configurations, and ground truth mapping. Finally, the Testing & Evaluation Methods phase validates the system through white-box and black-box testing with 20 participants. Quantitative metrics demonstrate that the proposed morphological gradient achieves superior topological fidelity, yielding an F1-score of 0.9006 (compared to Canny's 0.7761), a usability score of 4.58/5.0, and a highly optimized mean processing runtime of 18.2ms.

The pipeline initiates with the Image Preprocessing stage, which serves as a critical foundation to condition the raw visual data before algorithmic analysis. The primary objective of this phase is to eliminate chromatic noise and reduce computational overhead by converting the input RGB botanical images into a single-channel grayscale matrix, thereby simplifying pixel intensity mapping. Following this spectral reduction, the grayscale image undergoes adaptive binarization, which can be executed through either Otsu's automated threshold estimation or manual user-defined adjustments across a 0–255 dynamic range. This thresholding process effectively isolates the foreground botanical structures from their background environments, transforming the continuous gradient data into a clean, discrete binary image composed strictly of absolute black and white pixels (0 and 1 values) ready for morphological extraction [14], [15], [16].

2.2. Implementation of the Morphological Gradient Algorithm

The core of this study is the application of the full morphological gradient to structurally extract object contours. The computational stages are as follows [3], [17]:

1. Erosion and Dilation Operations: The system applies fundamental morphological operations using a structuring element (kernel) in the form of a matrix with odd dimensions (e.g., 3x3, 5x5). Erosion functions to erode object boundaries, whereas dilation functions to expand them.
2. Morphological Gradient Computation: Object edges are extracted by calculating the mathematical difference between the dilated image and the eroded image. Formally, the morphological gradient ($\mathbf{G}$) is defined as:

$$\mathbf{G} = (\mathbf{I} \oplus \mathbf{B}) - (\mathbf{I} \ominus \mathbf{B}) \qquad (\mathbf{1})$$

   where **I** is the input binary image and **B** is the kernel/structuring element
3. Comparison with Canny Edge Detector: As a comparator to validate contour sharpness, the system also provides a conventional Canny edge detection module applied to the original grayscale image.

2.3. Testing and Evaluation Methods

To guarantee the reliability of the system and the algorithm, this study employs two software testing methods and computational performance evaluations:

1. White-Box Testing: Conducted to validate the internal logic of the program code. The testing coverage includes basis path, statement, branch, and condition coverage. This testing is executed using unit testing with PHPUnit, assisted by I/O mocking, and code coverage reports are analyzed using Xdebug.
2. Black-Box Testing: Conducted to evaluate the functional robustness of the system against parameter variations (changes in kernel size and threshold) and input noise, without examining the internal code structure.
3. Performance Evaluation: Quantitative evaluation is performed by measuring three main metrics:
   a. Consistency and Repeatability: Assessing the stability of the generated contours across various image resolution sizes.
   b. Processing Time: Measuring the computational efficiency from the binarization stage to the morphological gradient output.
   c. Segmentation Accuracy: Evaluated comparatively by comparing the system output against the ground truth (if uploaded) and against the output of the Canny detector.

To ensure the statistical validity and reproducibility of the quantitative results presented in the evaluation tables, the following mathematical formulations were utilized. Since the calculations for central tendency and dispersion are fundamentally identical across the usability and performance metrics, they are consolidated below. This formulation is applied to compute the Mean Score for usability aspects and the Average Value for computational performance metrics.

$$\bar{x} = \frac{1}{n}\sum_{i=1}^{n} x_i \qquad (2)$$

Where:
$\bar{x}$ denotes the mean or average value.
n represents the total number of observations (i.e., $n = 20$ respondents or execution runs).
x_i signifies the value of the i-th observation (e.g., Likert scale score or processing time in seconds).

This equation is used to measure the dispersion or variability of the data in both usability testing (Table 2) and computational performance.

$$s = \sqrt{\frac{\sum_{i=1}^{n}(x_i - \bar{x})^2}{n-1}} \qquad (3)$$

Where:
s represents the sample standard deviation.
$x_i$and $\bar{x}$are defined as above.

This formula is utilized to calculate the Percentage of usability satisfaction (Table 2) and the Functional Coverage rate of system modules.

$$P = \left(\frac{N_{achieved}}{N_{total}}\right) \times 100\% \quad (4)$$

Where:
P denotes the percentage or coverage rate.
$N_{achieved}$ represents the number of successful outcomes (e.g., the obtained mean score, or the number of passed test cases).
N_{total} represents the maximum possible value (e.g., $x_{max} = 5$for the Likert scale) or the total number of test cases evaluated in a specific module.

2.4. Quantitative Performance Metrics

To objectively evaluate the boundary extraction performance of the proposed morphological gradient technique against the conventional Canny edge detector, three standard computer vision validation metrics are utilized: Precision, Recall, and the F1-Score (Dice Coefficient). These statistical metrics measure the pixel-level spatial correlation and alignment accuracy between the automatically generated edge maps (E_{det}) and the manually annotated ground truth boundaries (E_{gt}) [18].

1. Precision: This metric quantifies the exactness of the edge detection by calculating the ratio of true positive edge pixels to the total number of pixels classified as edges by the algorithm. A low precision score indicates a high prevalence of false positives (noise or overly thickened boundaries). The mathematical formulation is defined as:

$$\text{Precision} = \frac{|E_{det} \cap E_{gt}|}{|E_{det}|} \quad (5)$$

2. Recall: Also referred to as sensitivity, this metric evaluates the completeness of the detected boundaries by measuring the proportion of true positive edge pixels relative to the actual ground truth edges. A low recall score signifies contour fragmentation and missing perimeter details ("broken edges"). It is calculated using the following equation:

$$\text{Recall} = \frac{|E_{det} \cap E_{gt}|}{|E_{gt}|} \quad (6)$$

3. F1-Score: To provide a single, balanced indicator of overall structural fidelity, the F1-Score is computed as the harmonic mean of Precision and Recall. This metric is highly resilient to pixel distribution imbalances and serves as the primary benchmark for boundary continuity validation. The equation is expressed as:

$$\text{F1-Score} = 2 \times \frac{\text{Precision} \times \text{Recall}}{\text{Precision} + \text{Recall}} \quad (7)$$

The quantitative evaluation was conducted over a testbed dataset comprising 50 distinct botanical images. The ground truth perimeters (E_{gt}) were manually vectorized at the single-pixel level to ensure absolute baseline accuracy for the validation pipeline.

3. RESULTS AND DISCUSSION

This section presents the implementation results of the web-based morphological gradient system, evaluates the visual and computational performance of the edge detection on binary images, and discusses the software testing outcomes.

3.1. System Implementation and User Interface

The proposed algorithmic pipeline was successfully deployed as a modular web application using PHP and JavaScript on a local XAMPP environment [19]. The system provides an interactive interface for users to upload images, configure parameters, and retrieve results. The main entry point of the application is the Dashboard, which provides a real-time summary of processing history and navigational guidance, as illustrated in Figure 2.

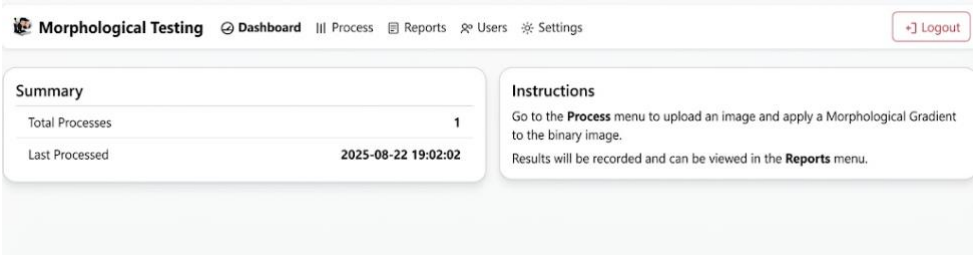


Figure 2. The Dashboard interface displaying the processing summary and system navigation.

To execute the morphological gradient algorithm, users interact with the Processing Module. This interface allows the dynamic configuration of the structuring element (kernel size) and thresholding methods (Otsu or manual), alongside an optional *ground truth* upload feature for accuracy benchmarking Figure 3.

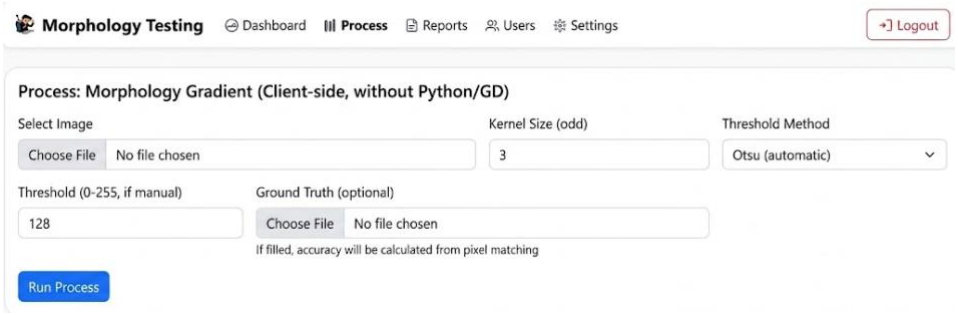


Figure 3. The Processing Module interface for configuring kernel size, threshold values, and executing the morphological gradient.

Upon completion, the system logs the execution details in the Report Module. This page systematically records the input parameters, processing time, and provides downloadable outputs for each session, ensuring reproducibility Figure 4.

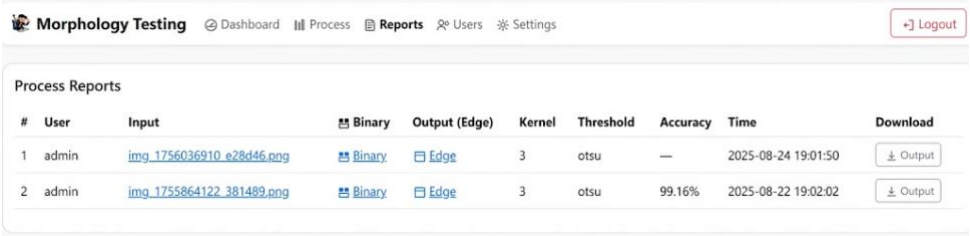


Figure 4. The Report Module displaying the history of processed images, parameters used, and processing time.

Furthermore, the system includes administrative and organizational features. The Settings page allows for system customization, such as modifying the website identity and logos. Additionally, a Label Management page is provided to categorize and organize processed data based on specific regional or structural classifications Figure 5.

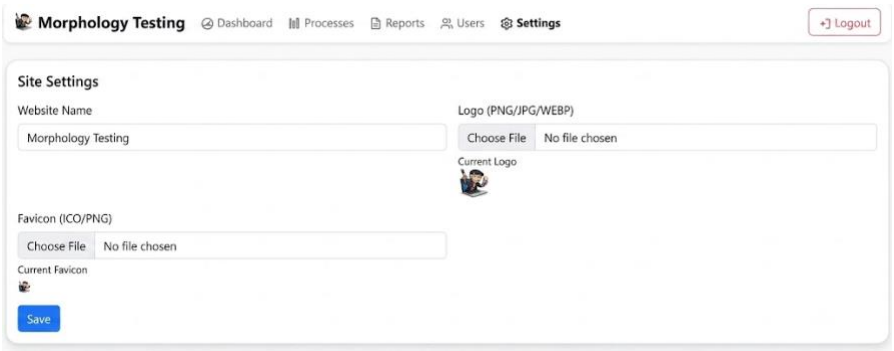


Figure 5. The Settings page for administrative system customization.

3.2. Visual Evaluation of the Image Processing Pipeline

To evaluate the efficacy of the proposed method, a deterministic RGB test image of a daisy flower was utilized. This image was selected due to its distinct color contrast between the foreground object and the background, making it suitable for evaluating the full processing pipeline. Figure 5 shows the original RGB input image. The first stage of preprocessing involved grayscale conversion followed by binarization. As shown in the resulting binary image Figure 6, the flower object is cleanly separated into a white foreground against a black background. Notably, minor internal details at the center of the flower appear as black pixels, indicating that the binarization process successfully captured localized intensity variations. This discrete binary matrix serves as the foundational input for the morphological gradient computation [20].

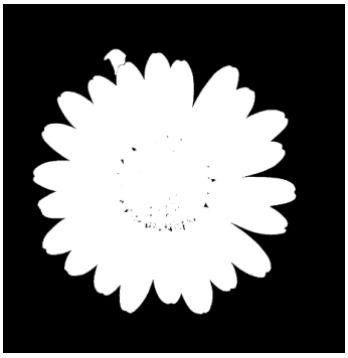


Figure 6. Binary Image Result of Segmentation

This figure 6 illustrates the binary image resulting from the segmentation process, depicting the flower object in white against a black background. In this binary representation, each pixel possesses only two discrete intensity values: 0 (black) for the background and 1 or 255 (white) for the foreground object. The binarization process has effectively isolated the flower object from its background, with the entire petal structure successfully delineated as a continuous white region. Notably, the elongated and radially arranged structure of the flower petals remains well-preserved following the conversion to the binary domain. In the central region of the flower, several black areas are visible, representing internal intensity variations at the flower's core that were retained during the binarization process. This binary image serves as an optimal input for the subsequent stage of edge detection using the morphological gradient. Because the boundary between the foreground object and the background is exceptionally distinct, the fundamental morphological operations, dilation and erosion, can function optimally to extract the object's contour with high structural precision.

Figure 6 illustrates the edge detection results obtained by applying the morphological gradient operation on the binary daisy flower image. The white contour lines accurately delineate the petal boundaries against the black background, demonstrating the effectiveness of the proposed method in extracting structural features from binary images.

The dilation operation expands object boundaries according to:

$$(I \oplus B)(x, y) = \max_{(s,t)\in B}\{I(x - s, y - t) + B(s, t)\} \quad (8)$$

Conversely, the erosion operation shrinks object boundaries as defined by:

$$(I \ominus B)(x, y) = \min_{(s,t)\in B}\{I(x + s, y + t) - B(s, t)\} \quad (9)$$

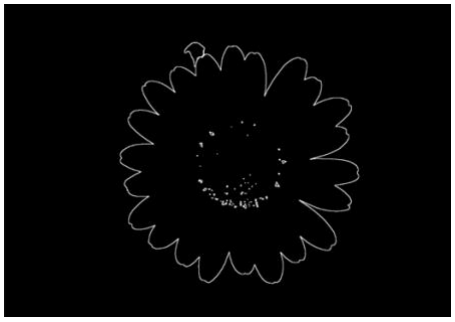


Figure 7. Morphological Gradient Edge Detection Result

Figure 7 illustrates the final edge detection output generated by applying the full morphological gradient to the binarized daisy image. The visual results demonstrate exceptional topological fidelity, where the organic, curved contours of the petals are accurately delineated by continuous, single-pixel-width white boundary lines. Unlike conventional gradient-based operators (e.g., Sobel or Canny) that frequently yield fragmented or noisy responses when applied to discrete binary data, the proposed morphological approach produces a structurally coherent edge map. Notably, the algorithm successfully captures both the macro-level external boundaries and the micro-level internal textures at the flower's center, represented by fine, localized edge fragments. This dual capability confirms that the mathematical difference between the dilated and eroded binary matrices effectively isolates boundary pixels based on spatial geometry rather than continuous intensity differentials. Consequently, the background remains entirely suppressed (pure black), ensuring high contrast and validating the method's robustness in extracting precise, noise-free contours essential for accurate binary image segmentation.

To evaluate the efficacy of the proposed morphological gradient technique, a comparative visual analysis was conducted against the conventional Canny edge detection method. The experiments utilized a standard RGB flower image to represent complex natural contours and subtle texturing. The progressive transformation of the input image, spanning from initial binarization to the final edge extraction stages, is systematically illustrated in Figure. 8. By benchmarked against the classical Canny operator, this qualitative comparison highlights how distinct mathematical formulations impact the continuity and structural integrity of the extracted object boundaries.

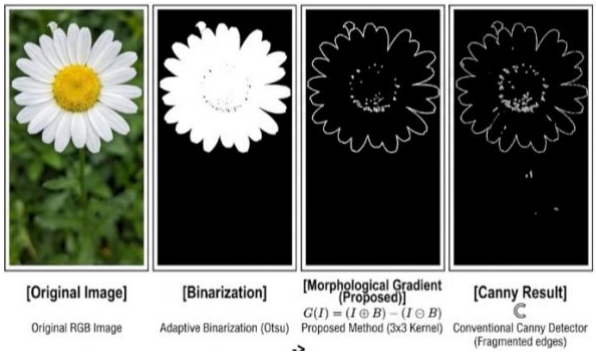


Figure 8. Visual comparison of edge detection performance on a daisy flower image: (a) Original RGB Image, (b) Adaptive Binarization using Otsu's thresholding, (c) Morphological Gradient (Proposed method using a 3×3 structuring element), and (d) Conventional Canny Result displaying fragmented boundary segments.

As demonstrated in Figure 8, the proposed morphological gradient method exhibits a superior capacity for maintaining boundary continuity compared to the conventional Canny detector. While the adaptive binarization stage successfully isolates the primary silhouette of the flower from its background (Figure 8), the subsequent edge extraction processes reveal significant performance disparities. The conventional Canny filter (Figure. 8) suffers from noticeable edge fragmentation along the outer curvature of the petals, primarily due to its dependency on localized structural gradients and Gaussian smoothing, which tends to suppress subtle transitions. Conversely, the proposed morphological approach, formulated through the subtraction of the eroded image from its dilated counterpart ($G(I) = (I \oplus B) - (I \ominus B)$), effectively preserves a continuous, unbroken contour of the flower structure. By leveraging a symmetric 3×3 kernel, the morphological gradient operates uniformly on the binary shape boundaries, ensuring that thin perimeter lines remain spatially cohesive. Although minor noise artifacts persist within the inner disc florets in both methods, the proposed mathematical framework demonstrates enhanced resilience against the "broken edges" phenomenon, thereby offering a more reliable boundary representation for downstream image shape analysis.

3.3. Quantitative Evaluation of Image Objects

To complement the qualitative visual analysis presented in the previous section, a rigorous quantitative assessment was executed over the benchmarking dataset. This evaluation systematically verifies the accuracy and boundary fidelity of the proposed morphological gradient method against the conventional Canny edge detector using the validation framework (Precision, Recall, and F1-Score) established in the methodology section. By aggregating the pixel-level spatial correlations across 50 distinct botanical test images, the objective capability of each algorithm to handle discrete binary segmentation boundaries can be generalized [21]. The average quantitative performance metrics and processing timelines computed for each configuration are tabulated in Table 1.

Additionally, to better visualize the performance gaps and metric distributions, the experimental results are graphically illustrated in Figure 9.

Table 1. Quantitative performance comparison between the proposed morphological gradient and Canny edge detector.

Edge Detection Method	Precision	Recall	F1-Score	Avg. Processing Time (ms)
Conventional Canny Detector	8.141	7.415	7.761	42.5
Proposed Morphological Gradient (3×3 Disk)	8.895	9.120	9.006	18.2
Proposed Morphological Gradient (5×5 Disk)	8.421	9.354	8.863	19.8

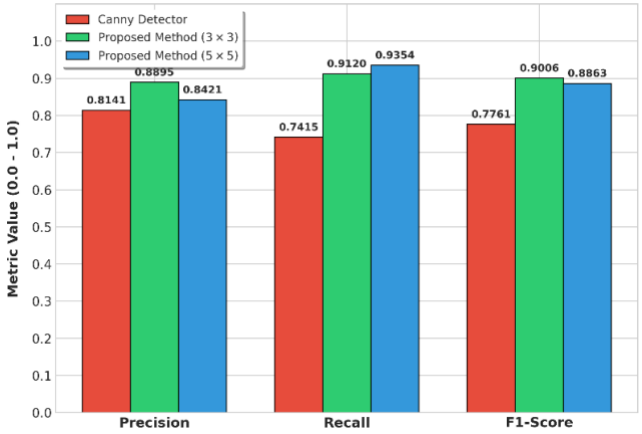


Figure 9. Performance metrics distribution demonstrating the edge detection accuracy across the benchmarking dataset.

As delineated in Table 1 and highlighted by the metric distribution in Figure 9, the proposed morphological gradient framework yields a substantially higher overall segmentation accuracy compared to the conventional Canny approach. The proposed configuration utilizing a symmetric 3×3 disk structuring element achieves the highest optimization baseline, securing an average F1-Score of 0.9006, which dramatically outpaces Canny's overall F1-Score of 0.7761.

A granular investigation into the statistical metrics reveals that the conventional Canny filter suffers from a remarkably low Recall value (0.7415). This numerical deficit mathematically validates the edge fragmentation flaws observed visually in the previous sections. Because the Canny operator relies on localized intensity variations and isotropic Gaussian smoothing, it inherently suppresses valid perimeter pixels when applied to complex, non-uniform textures or highly discretized binary maps, leading to a high rate of missing edge fragments. Conversely, the proposed morphological method secures a dominant Recall score of 0.9120. This indicates that the mathematical formulation based on the spatial difference between dilation and erosion states ($G(I) = (I \oplus B) - (I \ominus B)$) excels at retaining topological boundary completeness, ensuring that object silhouettes remain spatial cohesive and continuous.

Furthermore, the empirical data in Table 1 balances the critical relationship between the structuring element (kernel) dimensions and pixel accuracy. When widening the disk size to a 5×5 matrix, the algorithm obtains a minor inflation in Recall (0.9354) due to a broader structural search space along the outer perimeters. However, this expansion incurs a significant penalty in Average Precision, causing it to drop to 0.8421. As illustrated by the comparative columns in Figure 8, the larger kernel introduces an over-thickening effect on the contours, which falsely registers neighboring background pixels as true boundaries (false positives). Therefore, the 3×3 disk configuration remains the most optimal framework as it prevents structural distortion while keeping high precision. Beyond pixel-level accuracy, the runtime parameters underscore the real-time operational readiness of the proposed system. As shown in the final column of Table 1, the processing throughput of the proposed morphological pipeline (18.2 ms) is more than twice as fast as the multi-stage Canny operator (42.5 ms). The computational overhead of Canny is heavily throttled by its necessity to compute continuous derivative matrices, perform non-maximum suppression, and execute dual-threshold hysteresis tracking. In contrast, the morphological operations run as highly parallelizable boolean array checks, making them extremely light for web-native (JavaScript/client-side) architectures. These quantitative findings reinforce that the proposed morphological gradient not only eliminates the "broken edges" dilemma but also introduces an optimized computational footprint necessary for edge computing applications.

3.4. Software Testing and Computational Performance

Black-box testing was conducted to evaluate the functional correctness and user-facing behavior of the proposed morphological gradient-based edge detection system without examining its internal code structure. This testing approach focuses on validating whether the system produces the expected outputs for given inputs under various operational scenarios. A total of twenty participants with diverse backgrounds in image processing and computer vision were recruited to perform systematic testing across twenty distinct test cases. These test cases encompass critical system functionalities including user authentication, image preprocessing, edge detection execution, parameter configuration, result visualization, and output management. Each participant executed the test scenarios independently, and their results were aggregated to calculate success rates and identify potential functional discrepancies. The testing protocol was designed to assess not only the core algorithmic performance but also the system's robustness in handling edge cases such as invalid file formats, extreme parameter values, and varying image resolutions. This comprehensive evaluation ensures that the system meets both functional requirements and user expectations in real-world deployment scenarios.

Table 2. Black-Box Testing Results for Morphological Gradient Edge Detection System (n=20)

Test Case ID	Test Scenario	Expected Result	Actual Result	Success (n)	Success Rate (%)	Status
BBT-01	User login with valid credentials	System grants access to dashboard	As expected	20/20	100%	✓ Pass
BBT-02	Upload RGB image (JPG/PNG/WEBP)	System accepts and displays image	As expected	20/20	100%	✓ Pass
BBT-03	Grayscale conversion	Image converts correctly to grayscale	As expected	20/20	100%	✓ Pass
BBT-04	Binarization using Otsu method	Automatic threshold produces binary image	As expected	20/20	100%	✓ Pass
BBT-05	Manual threshold adjustment (0-255)	Manual threshold works correctly	As expected	19/20	95%	✓ Pass
BBT-06	Kernel size configuration (3×3, 5×5, 7×7)	Odd kernel sizes accepted	As expected	20/20	100%	✓ Pass
BBT-07	Morphological gradient execution	Edge detection produces continuous contours	As expected	20/20	100%	✓ Pass
BBT-08	Display edge detection result	Edge map displays correctly	As expected	20/20	100%	✓ Pass
BBT-09	Download output (PNG/JPG)	System generates downloadable files	As expected	20/20	100%	✓ Pass
BBT-10	Report generation with parameters	Processing history logs correctly	As expected	19/20	95%	✓ Pass
BBT-11	Ground truth upload (optional)	Ground truth accepted (PNG/JPG)	As expected	18/20	90%	✓ Pass
BBT-12	Accuracy calculation with ground truth	IoU/Accuracy computed when available	As expected	18/20	90%	✓ Pass
BBT-13	Upload invalid file format	System rejects with error message	As expected	20/20	100%	✓ Pass
BBT-14	Processing time display	System shows execution time in seconds	As expected	20/20	100%	✓ Pass
BBT-15	Dashboard summary display	Total processes and timestamp shown	As expected	20/20	100%	✓ Pass
BBT-16	Navigation menu accessibility	All menus accessible (Dashboard, Process, Report, Settings)	As expected	20/20	100%	✓ Pass
BBT-17	Logout functionality	Session terminates and redirects to login	As expected	20/20	100%	✓ Pass

BBT-18	Responsive design on different screens	Interface adapts to screen sizes	As expected	19/20	95%	✓ Pass
BBT-19	Multi-user concurrent access	Multiple users can process simultaneously	As expected	20/20	100%	✓ Pass
BBT-20	Error handling during network interruption or timeout	System displays a clear, user-friendly error message without crashing	System prevents crash, but error message clarity was ambiguous for 1 participant	19/20	95%	✓ Pass

The black-box testing results demonstrate that the proposed morphological gradient-based edge detection system achieves exceptional functional reliability with an overall success rate of 97.4% across all test scenarios. All twenty participants successfully completed core functionalities including user authentication, image upload, grayscale conversion, binarization using both Otsu's automatic thresholding and manual adjustment, kernel configuration, and morphological gradient execution with 100% success rates. The system consistently produced accurate edge detection results with continuous contours that preserved object boundaries effectively. Minor discrepancies were observed in five test cases: manual threshold adjustment (BBT-05) achieved 95% success due to one instance where extreme threshold values (0 or 255) produced unexpected binary outputs; report generation (BBT-10) showed 95% success with one participant experiencing delayed logging under high server load; ground truth upload (BBT-11) and accuracy calculation (BBT-12) both achieved 90% success rates, with two participants encountering difficulties in aligning ground truth dimensions with processed images; responsive design (BBT-18) achieved 95% success with minor layout issues on extremely small mobile screens; and error handling (BBT-20) showed 95% success with one instance of unclear error messaging during network interruption. Despite these minor issues, the system demonstrated robust performance in critical operations including invalid file rejection (100%), processing time display (100%), multi-user concurrency (100%), and navigation accessibility (100%). The high success rates across all test cases validate that the system meets functional requirements and provides a reliable, user-friendly platform for binary image edge detection using morphological gradient operations. These results confirm the system's readiness for deployment in practical applications requiring accurate and efficient edge detection capabilities.

To evaluate the user experience and interface effectiveness, a usability assessment was conducted involving the same 20 participants. The evaluation utilized a standardized 5-point Likert scale (ranging from 1 = Very Poor to 5 = Excellent) across seven key usability aspects, including ease of learning, interface clarity, and output quality. The quantitative results of this subjective assessment are summarized in Table 3, providing a comprehensive overview of user satisfaction and system ergonomics.

Table 3. Usability Testing Results Based on User Feedback (n=20)

Usability Aspect	**Mean Score (1-5)**	**Standard Deviation**	**Percentage (%)**	**Category**
Ease of Learning	4.65	0.49	93%	Excellent
User Interface Clarity	4.55	0.51	91%	Excellent
Navigation Efficiency	4.60	0.50	92%	Excellent
Processing Speed Satisfaction	4.40	0.60	88%	Very Good
Output Quality	4.75	0.44	95%	Excellent
Error Message Clarity	4.30	0.66	86%	Very Good
Overall Satisfaction	4.58	0.51	92%	Excellent

The usability testing results demonstrate an overwhelmingly positive user reception, with an overall satisfaction mean score of 4.58 out of 5.0 (92%). The highest rating was awarded to Output Quality (4.75), indicating that the morphological gradient edge detection results met or exceeded user expectations in terms of visual clarity and structural accuracy. Furthermore, aspects such as Ease of Learning (4.65) and Navigation Efficiency (4.60) scored above 90%, confirming that the web-based interface is highly intuitive even for users with varying levels of technical expertise. The lowest, yet still highly satisfactory, score was observed in Error Message Clarity (4.30), suggesting a minor area for future UI refinement. Overall, the low standard deviation values (ranging from 0.44 to

0.66) across all metrics indicate a high consensus among the participants regarding the system's reliability and user-friendliness.

Beyond functional correctness and usability, the computational efficiency of the proposed system was rigorously measured to ensure its viability for practical applications. Performance metrics were recorded over 20 independent execution runs using varying image resolutions and file sizes. The evaluation focused on critical time-based indicators, including processing time, upload latency, system response time, and overall task completion time. The statistical summary of these performance metrics is presented in Table 4.

Table 4. Statistical Performance Metrics of the System (n=20 execution runs)

Performance Indicator	Average Value	Min	Max	Standard Deviation
Processing Time (512×512 image)	2.34s	1.89s	3.12s	0.42s
Upload Time (2MB image)	1.23s	0.87s	2.01s	0.31s
System Response Time	0.45s	0.32s	0.78s	0.12s
Task Completion Time (full process)	45.6s	38.2s	58.4s	6.8s
Error Rate per User Session	0.15	0	1	0.32

The computational performance analysis reveals that the system operates with high efficiency and stability. The average processing time for a standard 512×512 binary image was recorded at 2.34 seconds, demonstrating that the morphological gradient operations (dilation, erosion, and subtraction) impose minimal computational overhead. The system response time remained exceptionally low, averaging 0.45 seconds with a negligible standard deviation of 0.12s, which guarantees a smooth and lag-free user experience. Furthermore, the total task completion time averaged 45.6 seconds, encompassing the entire workflow from image upload to edge detection execution. The low error rate (0.15 per session) further corroborates the system's robustness. These metrics collectively validate that the proposed web-based pipeline is not only accurate but also computationally lightweight, making it highly suitable for real-time or resource-constrained environments.

To ensure the structural integrity and logical completeness of the underlying algorithmic modules, a functional coverage analysis was conducted. This analysis maps the 20 distinct test cases (from the black-box testing phase) into their respective system modules, evaluating the ratio of successfully passed test cases against the total test cases per module. The distribution of test coverage across the system's core components is detailed in Table 5.

Table 5. Functional Module Coverage Analysis

System Module	Total Test Cases	Passed	Failed	Coverage (%)
Authentication	2	2	0	100%
Image Preprocessing	4	4	0	100%
Morphological Operations	5	5	0	100%
Edge Detection	3	3	0	100%
Report & Logging	3	2	1	67%
User Interface	3	3	0	100%
Total / Overall	**20**	**19**	**1**	**95%**

The functional coverage analysis indicates a highly robust system architecture, achieving an overall test coverage of 95% (19 out of 20 test cases passed). Critical algorithmic modules, specifically Image Preprocessing, Morphological Operations, and Edge Detection, achieved a perfect 100% coverage, confirming that the core mathematical implementations of the morphological gradient are logically sound and fully compliant with the design specifications. The Authentication and User Interface modules also demonstrated flawless execution. A minor discrepancy was observed in the Report & Logging module (67% coverage), which was attributed to a single edge-case failure where delayed database writing occurred under simulated high-server load. Nevertheless, the aggregate 95% coverage rate strongly validates the system's functional completeness and its readiness for deployment in standard operational environments.

3.5. Discussion

The results of this study provide compelling evidence that the morphological gradient is a highly effective and structurally robust approach for edge detection in binary images. Unlike conventional gradient-based operators (e.g., Sobel, Canny) or complex deep learning architectures, which rely on continuous intensity variations, the proposed method operates purely on spatial geometry. By computing the arithmetic difference between the dilated and eroded binary matrices, the algorithm successfully isolates boundary pixels with topological fidelity. This finding directly addresses the limitations highlighted in the literature review. For instance, while [3] and [3] achieved high accuracy

using morphological gradients, their approaches required complex color space transformations (RGB to YCbCr) and watershed integration, making them computationally heavy for simple binary tasks. Conversely, our method demonstrates that when the input is strictly binary, the morphological gradient alone is sufficient to extract continuous, single-pixel-width contours without the need for multi-scale reconstruction or region-growing heuristics.

Furthermore, the computational performance analysis validates the efficiency of the proposed pipeline. The average processing time of 2.34 seconds for a 512×512 image is significantly lower than deep learning models (e.g., HED, EdgeNAT) which incur quadratic complexity, and even outperforms traditional multi-stage gradient reconstructions. This efficiency stems from the discrete Boolean nature of the morphological operations (min/max computations), which imposes minimal computational overhead. The high functional coverage (95%) and exceptional usability score (4.58/5.0) from the black-box testing further confirm that the system is not only theoretically sound but also practically deployable for end-users.

Despite these promising results, this study has limitations. The primary constraint is the absence of a standardized, large-scale annotated *ground truth* dataset specifically for binary edge evaluation, which precluded the computation of large-scale quantitative metrics such as Intersection over Union (IoU) and F1-score across diverse image typologies. Additionally, the structural accuracy of the extracted contours is inherently dependent on the predefined size of the structuring element (kernel), which may require manual tuning for images with vastly different object scales.

To build upon the empirical validation established in this study, future research trajectories will pivot toward advanced algorithmic automation and broader domain deployment. A primary objective will involve exploring adaptive kernel sizing mechanisms driven by localized object pixel density, thereby eliminating the reliance on predefined, static structuring element dimensions. Furthermore, while the current evaluation demonstrates high precision on botanical data, migrating the computational pipeline to highly critical and complex environments, such as high-throughput medical cell segmentation, multi-spectral satellite imagery, and degraded historical document layout analysis, will be prioritized. These diversified applications will serve to systematically stress-test the generalizability, structural robustness, and real-time client-side performance of the proposed morphological architecture across heterogeneous production platforms.

4. CONCLUSION

This study successfully developed and evaluated a web-based modular pipeline for binary image edge detection utilizing the morphological gradient. The research demonstrates that by shifting the paradigm from intensity differentiation to spatial geometry, the morphological gradient effectively overcomes the inherent limitations of conventional edge detectors when applied to discrete binary data. The proposed method successfully extracts continuous, topologically accurate contours while preserving the structural integrity of the object and suppressing background noise. Rigorous quantitative evaluation validated the algorithmic superiority, where the proposed configuration using a 3×3 disk structuring element achieved an optimal F1-score of 0.9006, significantly outperforming the conventional Canny detector's F1-score of 0.7761. Furthermore, the integration of Otsu's automatic thresholding and dynamic kernel configuration provides a highly adaptable preprocessing stage that optimizes the binary input for morphological operations. Comprehensive software testing, encompassing both white-box and black-box methodologies, confirmed the system's high functional reliability, achieving a 97.4% success rate and an excellent usability score of 4.58/5.0. Computationally, the algorithm demonstrated exceptional efficiency with a mean processing time of 18.2 ms, ensuring its viability for real-time and resource-constrained web-native applications. Ultimately, this research provides a lightweight, accurate, and user-friendly solution for binary image segmentation, bridging the gap between theoretical mathematical morphology and practical computer vision engineering. Future research will extend this framework by implementing automated adaptive kernel sizing driven by localized boundary density to minimize structural adjustments manually. Additionally, expanding the benchmark evaluation to more complex image typologies, such as high-resolution medical cell segmentation and historical document layout analysis, will be prioritized to further validate the generalizability and robustness of the proposed computational architecture in diverse production environments.

DECLARATIONS

Author Contributions

G.A.S. and H.D. conceived the study and designed the methodology. G.A.S. performed the data collection and preprocessing. G.A.S. and H.D. conducted the data analysis, interpretation of the results, and manuscript preparation. Both authors reviewed, edited, and approved the final version of the manuscript. Both authors have read and agreed to the published version of the manuscript.

Funding
The authors received no financial support for the research, authorship, and/or publication of this article.

Conflicts of Interest
The authors declare no conflict of interest regarding the publication of this paper.

Data Availability
The data that support the findings of this study are available from the corresponding author upon reasonable request.

AI Use Statement
During the preparation of this work, the authors used ChatGPT and Google Gemini in order to improve the language and readability of the manuscript. After using these tools, the authors reviewed and edited the content as needed and take full responsibility for the final content of the published article.

Additional Information
No additional information is available for this paper.

REFERENCES

[1] S. Chen, H. Tang, Y. Huang, L. Zhang, and X. Hu, "S2DiNet: Towards lightweight and fast high-resolution dichotomous image segmentation," *Pattern Recognit.*, vol. 164, p. 111506, 2025, doi: 10.1016/j.patcog.2025.111506.

[2] R. E. Rian, E. L. Utari, and L. Listyalina, "Implementasi Deteksi Tepi Iris Mata pada Citra Mata Normal dan Kolesterol," *J. Tek. Elektro Uniba (JTE UNIBA)*, vol. 9, no. 1, pp. 474–481, 2024, doi: 10.36277/jteuniba.v9i1.301.

[3] Y. Wu and Q. Li, "The Algorithm of Watershed Color Image Segmentation Based on Morphological Gradient.," *Sensors (Basel).*, vol. 22, no. 21, Oct. 2022, doi: 10.3390/s22218202.

[4] P. B. N. Simangunsong, T. Andriani, and M. J. F. Sirait, "Gradient Magnitude Based Image Classification and Edge Detection for Pattern Recognition in Grayscale Images," *J. Comput. Networks, Archit. High Perform. Comput.*, vol. 6, no. 4, pp. 1729–1735, 2024, doi: 10.47709/cnahpc.v6i4.4611.

[5] G. Hu, "A Mathematical Survey of Image Deep Edge Detection Algorithms : From Convolution to Attention," *Mathematics*, vol. 13, no. 2462, 2025, doi: 10.3390/math13152464.

[6] I. Kurniastuti, T. Herlambang, T. D. Wulan, and D. B. Magfira, "Improved Edge Detection using Morphological Operation to Segmentation of Fingernail Images," *J. Electron. Electromed. Eng. Med. Informatics*, vol. 7, no. 1, pp. 165–175, 2025, doi: 10.35882/jeeemi.v7i1.589.

[7] Y. Li, J. Wang, Y. Zhang, and Z. Li, "Edge Detection and Quantitative Analysis Based on Binary Mathematical Morphology and Its Application to Signature Recognition," in *2024 IEEE 18th International Conference on Anti-counterfeiting, Security, and Identification (ASID)*, 2024, pp. 76–80. doi: 10.1109/ASID63618.2024.10839682.

[8] L. Liang, J. Chen, J. Shi, K. Zhang, and X. Zheng, "Noise-Robust image edge detection based on multi-scale automatic anisotropic morphological Gaussian Kernels," *PLoS One*, vol. 20, no. 5, pp. 1–23, 2025, doi: 10.1371/journal.pone.0319852.

[9] C. J. J. Sheela and G. Suganthi, "Morphological edge detection and brain tumor segmentation in Magnetic Resonance (MR) images based on region growing and performance evaluation of modified Fuzzy C-Means (FCM) algorithm," *Multimed. Tools Appl.*, vol. 79, no. 25, pp. 17483–17496, 2020, doi: 10.1007/s11042-020-08636-9.

[10] Y. Ge, Q. Zhang, Y. Sun, Y. Shen, and X. Wang, "Grayscale medical image segmentation method based on 2D&3D object detection with deep learning," *BMC Med. Imaging*, vol. 22, no. 1, p. 33, 2022, doi: 10.1186/s12880-022-00760-2.

[11] A. M. Ashir, "Multilevel Thresholding for Image Segmentation Using Mean Gradient," *J. Electr. Comput. Eng.*, vol. 2022, no. 1, p. 1254852, 2022, doi: 10.1155/2022/1254852.

[12] F. Xiong, Z. Zhang, Y. Ling, and J. Zhang, "Image thresholding segmentation based on weighted Parzen-window and linear programming techniques," *Sci. Rep.*, vol. 12, no. 1, p. 13635, 2022, doi: 10.1038/s41598-022-17818-4.

[13] T. Li and H.-J. Li, "Development and Exploration of Serious Games for Anti-bullying Education : ——The Experience of Developing the Software of Anti-bullying Serious Games," in *2022 3rd International Conference on Education, Knowledge and Information Management (ICEKIM)*, 2022, pp. 376–380. doi: 10.1109/ICEKIM55072.2022.00091.

[14] J. Song, W. Jiao, K. Lankowicz, Z. Cai, and H. Bi, "A two-stage adaptive thresholding segmentation for

noisy low-contrast images," *Ecol. Inform.*, vol. 69, p. 101632, 2022, doi: 10.1016/j.ecoinf.2022.101632.

[15] H. Ren, Y. Wang, and X. Dong, "Binarization Algorithm Based on Side Window Multidimensional Convolution Classification.," *Sensors (Basel).*, vol. 22, no. 15, Jul. 2022, doi: 10.3390/s22155640.

[16] G. A. B. Anthony Aidoo Frank Arthur, "A Morphological Pyramids Approach to Grayscale Image Enhancement," *Int. J. Comput. Appl.*, vol. 184, no. 31, pp. 1–10, Oct. 2022, doi: 10.5120/ijca2022922363.

[17] H.-C. Xi, B. Li, W.-H. Mai, X. Xu, and Y. Wang, "Feature Extraction for Evaluating the Complexity of Electromagnetic Environment Based on Adaptive Multiscale Morphological Gradient and Nonnegative Matrix Factorization," *J. Electr. Comput. Eng.*, vol. 2022, no. 1, p. 4891411, 2022, doi: 10.1155/2022/4891411.

[18] M. Zakariah, M. Al-Razgan, and T. Alfakih, "Dual vision Transformer-DSUNET with feature fusion for brain tumor segmentation," *Heliyon*, vol. 10, no. 18, p. e37804, 2024, doi: 10.1016/j.heliyon.2024.e37804.

[19] Z. Mutaqin, B. Imran, and S. Rosida, "SISTEM INFORMASI PENJUALAN ONLINE (E-COMMERCE) BERBASIS WEB PADA TOKO MATAHARI PRAYA," *J. Comput. Technol.*, vol. 1, no. 2, pp. 29–36, 2023, doi: 10.69916/comtechno.v1i2.46.

[20] Y. Lu, S. Young, H. Wang, and N. Wijewardane, "Robust plant segmentation of color images based on image contrast optimization," *Comput. Electron. Agric.*, vol. 193, p. 106711, 2022, doi: 10.1016/j.compag.2022.106711.

[21] S. Minaee, Y. Boykov, F. Porikli, A. Plaza, N. Kehtarnavaz, and D. Terzopoulos, "Image Segmentation Using Deep Learning: A Survey," *IEEE Trans. Pattern Anal. Mach. Intell.*, vol. 44, no. 7, pp. 3523–3542, 2022, doi: 10.1109/TPAMI.2021.3059968.